Cardio-Respiratory Phase Synchronization from Reconstructed Respiration

A. Kuhnhold, A.Y. Schumann, R.P. Bartsch, G. Schmidt, and J.W. Kantelhardt

***Abstract*—Changes in the phase-synchronization behavior of a physiological system can characterize the complexity of its dynamics. Taking the human cardio-respiratory system as an example and using a recently developed procedure for an automated screening of synchrograms we study the data of 874 post-infarction patients, where heartbeat intervals and respiration were recorded approximately one week after the index myocardial infarction event. We find that phase synchronization is decreased in patients with increased mortality risk or age. However, our analysis also indicates that data from 30 minutes recordings is insufficient to achieve a reliable statistics for predicting mortality risk based on phase synchronization. Therefore, we further develop techniques for extracting respiratory information from ECG recordings to be able to use long-term Holter recordings of post-infarction patients in future studies. In particular, we compare breathing-phase reconstructions based on the amplitude of the R peaks in the ECG or beat-to-beat time intervals with real respiratory phases.**

***Index Terms*—heart rate, respiration, phase synchronization, synchrogram, post-infarction patients, mortality risk**

I. Introduction

Transitions in the synchronization behavior of coupled oscillators have been shown to be important characteristics of model systems [1]. However, phase synchronization is difficult to study in experimental data which are very often inherently nonstationary and thus contain only quasiperiodic oscillations.

In physiology, the study of phase synchronization focuses on cardio-respiratory data and encephalographic data [2]. First approaches for the study of cardio-respiratory synchronization have been undertaken by the analysis of the relative position of inspiration within the corresponding cardiac cycle [3]. More recently, phase synchronization between heartbeat and breathing has been studied using the synchrogram method [1], [4]–[7]. While long synchronization episodes were observed in athletes and heart-transplant patients (several hundreds of seconds) [4], [5], shorter episodes were detected in normal subjects (typical duration less than hundred seconds) [5]–[8]. In this paper, we use the recently developed automated procedure [7], [9] for screening the cardio-respiratory synchrograms of 874 post-infarction patients, where heartbeat intervals and respiration were recorded approximately one week after an index myocardial infarction event.

A.K. and J.W.K. are with the Institute of Physics, Martin-Luther-University Halle-Wittenberg, Germany, email: jan.kantelhardt@physik.uni-halle.de

A.Y.S. is with the Complexity Science Group at the Department of Physics and Astronomy, University of Calgary, Canada

R.P.B. is with Harvard Medical School and Division of Sleep Medicine, Brigham and Women's Hospital, Boston, USA

G.S. is with the 1. Medizinische Klinik, Technical University Munich, Germany

The risk to die of sudden cardiac death (SCD) was shown to be significantly increased after an acute myocardial infarction [10]. Studies in high-risk survivors have reported a reduced mortality due to the implantation of an implantable cardioverter defibrillator device [11]. Thus, the identification of post-infarction patients at risk of SCD is a crucial element in post-infarction therapy and surgery. Besides the currently used gold standard for mortality-risk assessment, left ventricular ejection fraction (LVEF), several other predictors and scores have been suggested [12] including deceleration capacity (DC) describing the heart's capability to decelerate [13], [14]. A very recent study utilized a reduced respiratory sinus arrhythmia (RSA) among high-risk patients for risk assessment [15].

However, RSA, that is the modulation of the heart rate due to respiration [16] must be distinguished from synchronization. In RSA, respiration influences the sympathovagal balance of the autonomous nervous system and, thus, affects heart rate. While a sympathetic predominance during inspiration causes the heart to accelerate (shorter beat-to-beat intervals), expiration enhances vagal tone and suppresses sympathetic output yielding a reduction in heart rate, i.e., a prolongation in beat-to-beat intervals. The actual times of the individual heartbeats, however, must not be correlated with the respiratory cycle. For phase synchronization, on the other hand, heartbeats occur at specific phases of the respiratory oscillator.

In this paper we apply the automated synchrogram screening procedure [7], [9] to the data of 874 post-infarction patients, and compare results for real and reconstructed respiration. We tackle the question to which extent cardio-respiratory phase-synchronization can be studied using respiration reconstructed from heartbeat and discuss the usability of phase-synchronization for mortality-risk assessment.

II. Data and Methods

A. Measurements and Preprocessing

From 874 survivors of an acute myocardial infarction 3-lead high-resolution electrocardiogram (1600Hz), blood pressure, and thorax excursion were recorded for 30 minutes. All recordings were obtained within the second week after the index infarction event in supine position under resting conditions. For measuring ECG signals we used the orthogonal bipolar Frank-leads [see Fig. 1(a)] with back-to-front component X, right-to-left component Y, and foot-to-head component Z. ECG data was preprocessed using the QRS-complex detection software Librasch [17]. Identified heartbeats and their classification, i. e., normal beat, ectopic beat, or artifact, were checked by trained personnel. We consider the times $t_k, k = 1, \ldots, N$ of R peaks as a proxy for heartbeat times and derive the

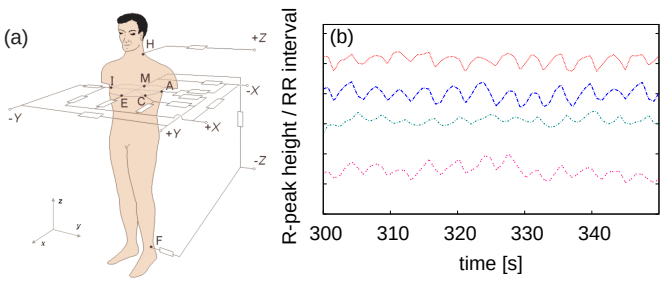

Fig. 1. (a) Illustration of Frank leads setup (taken from [20]). (b) R-peak amplitudes and R-R intervals from ECG signals recorded from a post-infarction patient; from top to bottom: Frank-leads X (red), Y (blue), and Z (turquoise), as well as the RRI signal (pink).

signal of beat-to-beat time intervals (RRI) from the ECG-lead containing the least artifacts (see Fig. 1(b), bottom curve). While we keep ventricular and super-ventricular beats, artifacts are excluded. In addition, we calculate the amplitudes of the R peaks from all three leads (see Fig. 1(b), three top curves). Thorax excursion was monitored by stretch sensors incorporated in an elastic belt around the thorax. Finally, all five time series (three R-peak signals, RRI, and thorax excursion as proxy of real respiration) are resampled to 4Hz by a linear interpolation of the values.

B. Calculation of Respiratory Phase Signals

In order to obtain a phase signal for the real-respiration recording, $x(t)$, we employ the analytical signal approach by complementing $x(t)$ with its complex counterpart $i\tilde{x}(t)$ that is defined via a Hilbert transform [18]

$$\tilde{x}(t) = \frac{1}{\pi}\text{P.V.}\int_{-\infty}^{\infty}\frac{x(t')}{t-t'}dt' \,. \tag{1}$$

Here, P.V. denotes the Cauchy principal value. From the analytical signal expression

$$\hat{x}(t) = x(t) + i\tilde{x}(t) = A(t)e^{i\varphi(t)} \tag{2}$$

follow both the instantaneous amplitude signal, $A(t) = \sqrt{x^2(t)+\tilde{x}^2(t)}$, and the instantaneous phase signal, $\varphi(t) = \text{atan2}\{\tilde{x}(t), x(t)\}$. The Hilbert transform in Eq. (1) requires two prerequisites in order to result in meaningful amplitude and phase signals: (i) the input signal, $x(t)$, must oscillate around zero which can be guaranteed by subtracting its mean value $\langle x\rangle = N^{-1}\sum_{l=1}^{N} x(l\Delta t)$ with $\Delta t = 0.25s$, and (ii) a narrow frequency band which is ensured by incorporating a bandpass frequency filter, e.g., confining frequencies to the HF band $(0.15-0.4\text{Hz})$ in the case of respiration. In practice the Hilbert transform can easily be computed by applying the convolution theorem: We rewrite Eq. (1) as the product of the Fourier transform of $1/(\pi t)$, being $-i\,\text{sgn}(f)$ with frequency f, and the Fourier transform of $x(t)$. We further denote by $\varphi_{\text{real resp}}(t)$ the phase signal calculated from thorax excursion.

C. Reconstructing Respiration from ECG Data

Our *first* reconstruction method exploits the variation of the axis of the heart caused by respiration and resulting in a modulation of R-peak amplitude. This means, the envelope

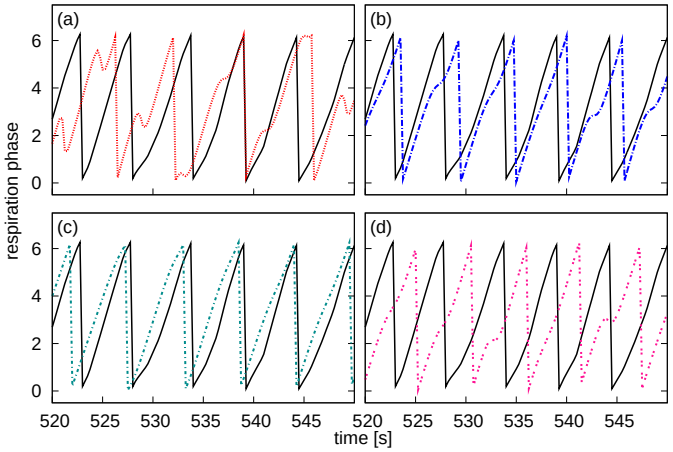

Fig. 2. Comparison of phases for real respiration (black, solid line) and four types of reconstructed respiration (dotted curves, colors correspond to those in Fig. 1) in a randomly chosen subject. (a)-(c) Reconstruction from the ECG-leads after Frank: (a) X, (b) Y, and (c) Z; (d) reconstruction from RR intervals. The reconstruction shown in (c) is best, i.e., the phase difference between real and reconstructed respiration is most stable.

of the raw ECG, using the (resampled) R-peak amplitudes as nodes, can serve as a respiration proxy. We calculate from all three resampled R-peak amplitude signals, $x^{(j)}(t)$ with $j = X, Y, Z$ indicating the Frank leads, the instantaneous amplitude functions (reconstructed breathing signals), $A^{(j)}(t)$, and the instantaneous phase signals, $\varphi^{(j)}_{\text{rec resp}}(t)$. For this we employ Fourier filtering, i. e., transforming the resampled signal to frequency space by a fast Fourier transform (FFT), applying a bandpass filter adjusted to HF components, and transforming back to time space by an inverse FFT. The filter works best if a Gaussian bandpass with center 0.35 Hz and width (standard deviation) 0.10 Hz is used [19]. Finally, an analytical signal approach following Eq. (2) yields the reconstructed respiratory phases. Examples of the phases $\varphi^{(X)}_{\text{rec resp}}(t)$, $\varphi^{(Y)}_{\text{rec resp}}(t)$, and $\varphi^{(Z)}_{\text{rec resp}}(t)$ are depicted in Fig. 2(a-c) together with the phase $\varphi_{\text{real resp}}(t)$ of real respiration.

The *second* reconstruction method exploits the RSA mechanism. Respiratory components can be extracted from a RRI time series by Fourier filtering and an analytical signal approach as described above. Note that the strength of RSA effects varies among subjects, and there are subjects where RSA can not be used to extract respiration from heartbeat data, see [9] for discussion. After reconstructing respiration from heartbeat intervals we calculate a phase signal, $\varphi^{(RRI)}_{\text{rec resp}}(t)$, according to Eq. (2). Figure 2(d) shows $\varphi^{(RRI)}_{\text{rec resp}}(t)$ together with $\varphi_{\text{real resp}}(t)$ for a typical post-infarction patient.

D. Quantifying Phase Synchronization

Our algorithm for the detection of phase-synchronization episodes is based on the study of cardio-respiratory synchrograms [1], [4]–[6]. For each record, the times t_k of heartbeats are mapped on the continuous cumulative phases $\varphi(t)$ of the respiratory signal, considering both, real and reconstructed respiratory phases. Figures 3(a,b) show representative synchrograms for both cases, where $\varphi(t_k) \bmod 2\pi$ is plotted versus t_k. In case of n:1 synchronization (i. e., if n heartbeats occur

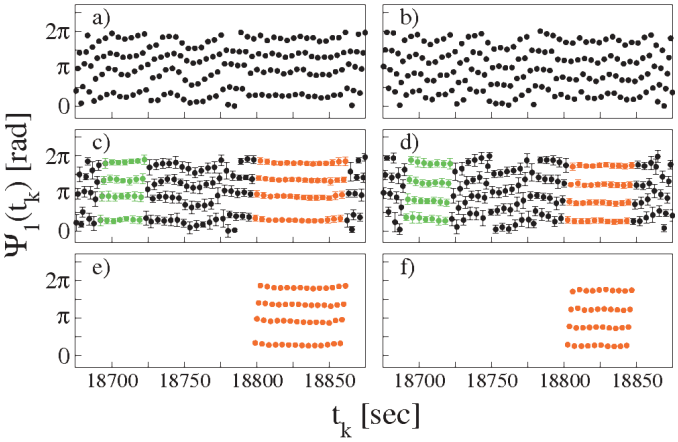

Fig. 3. Examples illustrating the automated synchrogram method for real [left] and reconstructed [right] respiration signals of the same subject during the same period of time. Symbols in (a,b) show the instantaneous respiratory phases at the time of the heartbeats. (c,d) means and standard deviations of the phases, calculated in time intervals of length $\tau = 30$s around each point in the horizontal lines. (e,f) Phase points with a standard deviation larger than the threshold $\delta = 5$ were deleted and then sequences shorter than the threshold T were also deleted. Red and green marked elements fulfill the standard deviation criterion, but sequences in green being shorter than the minimal duration T are deleted. Note that T must be slightly smaller for reconstructed breathing [right], since the continuous segments are shorter.

within one breathing cycle) one observes n parallel horizontal lines in the synchrogram [$n = 3$ in Figs. 3(a,b)]. In general, to find different ratios n:m of phase synchronization, we plot $\Psi_m(t_k) = \varphi(t_k) \bmod 2\pi m$ versus t_k.

While most earlier work relies on a visual evaluation of the synchrograms [4], [6], we detect the episodes in a fully automated way. For each synchronization ratio n:m we first replace the n phase points $\Psi_m(t_k)$ in each m respiratory cycles by the averages $\overline{\Psi}_m(t_k)$ calculated over the corresponding points in the time windows from $t_k - \tau/2$ to $t_k + \tau/2$ [Figs. 3(c,d)]. In the second step, the algorithm deletes all phase points $\overline{\Psi}_m(t_k)$ where the mean standard deviation of the n points in each m breathing cycles, $\langle\sigma\rangle_n$, is larger than $2m\pi/n\delta$. In the third step, only the phase points $\overline{\Psi}_m(t_k)$ in uninterrupted sequences of durations exceeding T seconds are kept [Figs. 3(e,f)]. Two examples for the detection of higher order cardio-respiratory synchronization are shown in Fig. 4.

A comparison of the detected synchronization rates in real data and in surrogate data has been used to optimize the parameters δ and T. We found that $\delta = 5$ and $T = 30$s [7] and $T = 25$s are best for real and reconstructed respiration, respectively. We note that changing the parameter δ has a similar effect on the results as changing T. Our results do hardly depend on the duration τ of the initial running average.

E. Deceleration Capacity

To study changes of cardio-respiratory phase synchronization with the mortality risk of the patients we calculate deceleration capacity (DC) by *phase rectified signal averaging* (PRSA) [13], [14]. In the PRSA algorithm (i) anchors at positions ξ are selected in the RRI signal (x_i) for moderate decelerations ($x_{\xi-1} < x_\xi < 1.05x_{\xi-1}$), and (ii) the surroundings of each anchor are then averaged with respect to the anchor

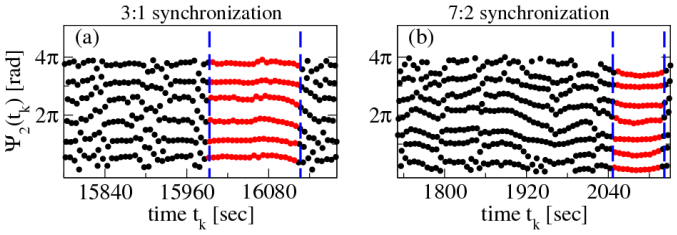

Fig. 4. Higher order cardio-respiratory phase synchronization studied by the automated synchrogram method for $m = 2$ with marked phase-synchronized episodes (red) versus time. Blue dashed lines mark the beginning and the end of the synchronized episodes. In (a) $6:2 = 3:1$ synchronization is observed while (b) illustrates a $7:2$ episode.

position ξ to obtain the PRSA signal $\bar{x}(i)$. DC is defined by $\mathrm{DC} = \frac{1}{4}\big[\bar{x}(0) + \bar{x}(1) - \bar{x}(-1) - \bar{x}(-2)\big]$. $\mathrm{DC} \leq 2.5$ms was associated with high mortality risk, $2.5\text{ms} < \mathrm{DC} \leq 4.5$ms with intermediate risk, and $\mathrm{DC} > 4.5$ms with low risk [13].

III. Results and Discussion

Comparing the two methods to reconstruct respiration from ECG recordings we found that for a vast majority (approx. 94%, depending on the filter parameters) of post-infarction patients a reconstruction based on R-peak amplitude outperforms a reconstruction based on beat-to-beat time intervals [19]. This implies that the cardio-respiratory coupling is rather characterized by peak-amplitude modulations than by frequency modulations (RSA effects). Although, different ECG leads seem to be optimal for a peak-amplitude based reconstruction of respiration for different individuals, differences are negligible and multi-lead ECG recordings are only necessary for applications which require high reliability. We are convinced that ECG based reconstruction of breathing is particularly interesting for sports medicine applications or sports instruments used for training purposes where belt measurements are disturbing, e. g., portable monitoring devices used by cyclists, runners, or alpinists to keep track of their own performance or to avoid health-threatening events caused by overexertion and overtraining. Moreover, there is an ongoing demand of more portable sleep-monitoring systems which can be distributed to a larger group of patients and controls at home enabling statistically more reliable large scale studies.

Our results from studying n:1 and n:2 cardio-respiratory coupling, for each patient using real respiration and the optimal breathing reconstruction are depicted in Fig. 5. The figure shows the percentages of time with detected synchronization; this corresponds approximately to the percentages of heartbeats and the percentages of breaths with observed synchronization. We find that the overall cardio-respiratory phase-synchronization is systematically larger for reconstructed breathing. However, the distribution is preserved. We suspect this effect is caused by an 'additional harmonic denoising' of the signals due to the methodology.

Table I lists the average percentages of synchronized time for subgroups of patients and real respiration as well as reconstructions from R-peak amplitudes and RR intervals. One can see that the percentages of synchronized time hardly depend on age except for a significant decrease in advanced age. This

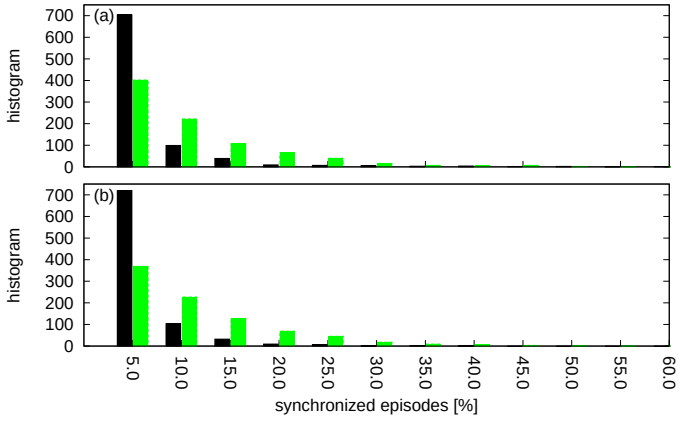

Fig. 5. Histograms of the ratios (percentages) of synchronized time for (a) n:1 and (b) n:2 cardio-respiratory phase synchronization, comparing results of real (black bars) and reconstructed (green bars) respiration in all subjects.

pattern is observed in the same way with similar significance levels for real respiration and both types of reconstructed respiration. Thus, also the absolute values are much larger for reconstructed respiration, differences between the patients and aging effects are well recovered. In general, the aging effect seems to be stronger regarding $n:1$ synchronization than regarding $n:2$ synchronization.

The second part of Table I shows that the percentages of synchronized time are strongly correlated with DC, which is a powerful predictor of mortality after myocardial infarction and is more accurate than LVEF and the conventional measures of heart-rate variability [13]. Phase synchronization can distinguish all three mortality-risk classes defined by DC for both reconstruction methods. The low significance levels in comparing the high-risk class (DC$<$2.5ms) and the intermediate risk (2.5ms$\leq$DC$<$4.5ms) class are due to the low number of patients in these classes and the rare occurrence of reliable phase-synchronization events. Therefore, if we want to use phase-synchronization parameters to determine the individual risk for each patient longer recordings with more synchronization episodes must be studied to get more reliable synchronization percentages for each patient.

TABLE I

AGE AND DC DEPENDENCE OF CARDIO-RESPIRATORY PHASE SYNCHRONIZATION FOR REAL RESPIRATION AND ITS RECONSTRUCTION CHARACTERIZED BY THE PERCENTAGES OF TIME FOR n:1 AND $n:2$ SYNCHRONIZATION. PROBABILITIES OF EQUIVALENT MEANS IN EACH SUBGROUP AND THE NEXT SUBGROUP EMPLOYING A T-TEST ARE INDICATED BY SYMBOLS: $p < 0.001$ ($\ddagger$), $p < 0.01$ ($\dagger$), AND $p < 0.03$ ($\star$). AGES $\geq$ 70YRS ARE COMPARED WITH $<$ 50YRS , AND DC $>$ 4.5MS WITH $0 <$ DC $\leq$ 2.5MS.

	heartbeat vs.	real respiration		best R-peak amplitude		RR interval	
	box-filter [0.16Hz-0.51Hz]	n:1	n:2	n:1	n:2	n:1	n:2
age [yrs]	< 50	4.0	3.4	9.3	9.2	3.9	3.7
	$50-59$	4.0	2.9	9.5	8.7	3.8*	3.4
	$60-69$	3.1†	2.5	8.1‡	8.3	2.6*	2.8
	≥ 70	2.0‡	2.3*	5.7‡	7.3*	1.8‡	2.8‡
DC [ms]	0$<$DC$\leq$2.5	1.5*	2.1	3.9†	6.0	0.6‡	1.5
	2.5$<$DC$\leq$4.5	2.2‡	2.1‡	5.8‡	6.7‡	1.2‡	1.6‡
	4.5$<$DC$<$12	4.5‡	3.4†	10.9‡	10.2‡	4.4‡	4.0‡

IV. CONCLUSION

We have investigated cardio-respiratory coupling using the recently suggested automated synchrogram screening method [7]. We found that a larger average phase synchronization is observed for reconstructed respiration compared with real respiration. Our results from comparing phase synchronization to a mortality-risk related index indicate that a reduced cardio-respiratory coupling correlates with high-mortality risk. Hence, phase-synchronization might complement established risk scores. However, the relatively short overall duration of synchronous episodes (just a few percent of the total recording time) shows that recordings longer than 30 minutes are needed to derive actual risk predictors from phase-synchronization. We are currently testing our hypotheses for 24h recordings.

ACKNOWLEDGMENT

We acknowledge financial support from the European Union project SOCIONICAL and R.P.B. particularly thanks the German Academic Exchange Service (DAAD) for funding.

REFERENCES

[1] M. G. Rosenblum, A. Pikovsky, C. Schäfer, P. A. Tass, and J. Kurths, in: *Handbook of Biological Physics* **4**, ed. S. Gielen and F. Moss:p. 279, Elsevier, New York, 2001; A. Pikovsky, M. Rosenblum, and J. Kurths, *Synchronization – A universal concept in nonlinear science*, Cambridge University Press, 2001.

[2] P. Tass et al., *Phys. Rev. Lett.*, **81**:3291, 1998; L. Angelini et al., *Phys. Rev. Lett.*, **93**:038103, 2004.

[3] P. Engel, G. Hildebrandt, and H.G. Scholz, *Pflügers Arch.*, **298**:259, 1967; H. Passenhofer and T. Kenner, *Pflügers Arch.*, **355**:77, 1975; F. Raschke, in: *Temporal Disorder in Human Oscillatory System*, edited by L. Rensing *et al.*:pp. 152, Springer, Berlin, 1987.

[4] C. Schäfer, M.G. Rosenblum, J. Kurths, and H.-H. Abel, *Nature*, **392**:239, 1998; *Phys. Rev. E*, **60**:857, 1999.

[5] E. Toledo, S. Akselrod, I. Pinhas, and D. Aravot, *Med. Eng. Phys.*, **24**:45, 2002.

[6] M.B. Lotric and A. Stefanovska, *Physica A*, **283**:451, 2000; A. Stefanovska, H. Haken, P. V. E. McClintock, M. Hozic, F. Bajrovic, and S. Ribaric, *Phys. Rev. Lett.*, **85**:4831, 2000; M.-Ch. Wu and Ch.-K. Hu, *Phys. Rev. E*, **73**: 051917, 2006.

[7] R. Bartsch, J. W. Kantelhardt, T. Penzel, and S. Havlin, *Phys. Rev. Lett.*, **98**:054102, 2007.

[8] M.D. Prokhorov, V.I. Ponomarenko, V.I. Gridnev, M.B. Bodrov, and A.B. Bespyatov, *Phys. Rev. E*, **68**:041913, 2003.

[9] C. Hamann, R. P. Bartsch, A. Y. Schumann, T. Penzel, S. Havlin, and J. W. Kantelhardt, *Chaos*, **19**:015106, 2009.

[10] H. V. Huikuri, A. Castellanos, and R. J. Myerburg, *N. Engl. J. Med.*, **345**:1473–1482, 2001; A. E. Buxton, *J. Cardiovasc. Electrophysiol*, **16**:S25–S27, 2005.

[11] A. J. Moss et al., *N. Engl J. Med.*, **335**:1933–1940, 1996; ibid **346**:877–883, 2002.

[12] H. V. Huikuri, J. S. Perkiomaki, R. Maestri, and G. D. Pinna, *Phil. Trans. R. Soc. A*, **367**:1223–1238, 2009.

[13] A. Bauer et al., *Lancet*, **367**:1674, 2006.

[14] J. W. Kantelhardt, A. Bauer, A. Y. Schumann, P. Barthel, R. Schneider, M. Malik, and G. Schmidt, *Chaos*, **17**(1):015112, 2007.

[15] M. Peltola, M. P. Tulppo, A. Kiviniemi, A. J. Hautala, T. Seppanen, P. Barthel, A. Bauer, G. Schmidt, H. V. Huikuri, and T. H. Makikallio, *Ann. Med.*, **40**:376–382, 2008.

[16] F. Yasuma and J. Hayano, *Chest*, **125**:683–690, 2004.

[17] R. Schneider, Opensource QRS detector, `www.librasch.org`, 2005.

[18] D. Gabor, *Radio Commun. Eng.*, **93**:429, 1946; B. Boashash, *Proc. IEEE*, **80**:520–538, 1992.

[19] A.Y. Schumann, A. Kuhnhold, K. Fuchs, R.P. Bartsch, A. Bauer, G. Schmidt, and J.W. Kantelhardt, Proceedings of the 6th ESGCO 2010.

[20] J. Malmivuo and R. Plonsey, *Bioelectromagnetism - Principles and Applications of Bioelectric and Biomagnetic Fields* (Oxford University Press, 1995); also available at http://www.bem.fi/book/.